ELSEVIER

Journal of Chromatography A, 743 (1996) 33–42

JOURNAL OF CHROMATOGRAPHY A

Apparent pore size distributions of chromatography media

Lars Hagel*, Magnus Östberg, Torvald Andersson

R&D Department, Pharmacia Biotech AB, S-751 82 Uppsala, Sweden

Abstract

The use of size-exclusion chromatography for determination of pore dimensions of chromatography media is reviewed. It is noted that many researchers still use the simple but inaccurate method of treating the selectivity curve as a cumulative pore size distribution. An alternative procedure for estimation of pore dimensions of media through iteration of the apparent pore size distribution to yield elution data in agreement with experimental data for polymers of known hydrodynamic radius using a simple spread sheet is presented. Data of apparent pore dimensions of some commercial media for aqueous size-exclusion chromatography is presented. The influence of various parameters, e.g., solute shape, pore shape, method errors, etc., is discussed. It is concluded that size-exclusion chromatography can not provide information about the pore structure and, thus, the pore size obtained is dependent upon the selected pore model.

Keywords: Pore size distribution; Stationary phases, LC; Dextrans

1. Introduction

The fact that retention volume in size-exclusion chromatography (SEC) is affected by the size of the solute, as well as by the pore dimensions of the matrix was realized already when the first gel filtration experiments were conducted in the late 1950s [1–3]. The possibility of using SEC for obtaining information about the structure of the matrix was soon explored [4]. Aggebrandt and Samuelsson proposed that poly(ethylene glycol) of varying molecular mass could be used to elucidate the pore size distribution in cellulose fibers [5].

It was also early noted that there is no one-to-one relationship between the selectivity curve of the gel and the pore size distribution and this was attributed to ratio of pore size to solute size [6,7]. Unfortunately, many researchers have overlooked this fundamental observation. The physical explanation behind the observation is the so called "wall effect", i.e., the fact that the center of the molecule is excluded from a volume close to the wall due to the size of the molecule [6]. This is the reason why also a single pore size support will separate molecules according to size, i.e., the accessible pore volume is restricted by the size of the molecules themselves. In principle, a failure to account for the "wall effect" will lead to the erroneous assumption that the selectivity curve is equal to the pore size distribution curve [8]. This will yield an apparent pore size distribution (PSD) of narrower width and lower average than the PSD obtained by, e.g., mercury porosimetry.

However, the procedure is simple and a number of methods based upon this assumption has been published [9–20]. In one of the first studies describing the use of SEC to obtain pore size data Halász found that he needed to assign a size of 2.7-times the real size of polystyrene to get data for average pore size in accordance with absolute methods [9]. Thus this method relies on a calibration of the molecular size to yield an estimate of average pore size but this will

*Corresponding author.

S0021-9673/96/$15.00 © 1996 Elsevier Science B.V. All rights reserved
PII S0021-9673(96)00130-6

of course only be valid for the system at hand and furthermore will not yield any reliable information about the distribution of pore size. Kuga [17] used the same assumption to calculate the pore size distribution of materials from a batch mode but without the correction of solute size. However, he noted the shortcomings of the method but still promoted it as a crude method for obtaining the PSD. Ackers [21] used the selectivity curve to describe the random distribution of penetrable volume fractions to describe a calibration procedure. It is interesting to note his concluding remark: "It would appear that, whereas the models used in deriving column calibration functions are useful in determining molecular sizes, they should not be taken as true structural representations of the gel matrix." In spite of this comment several authors have interpreted the distribution of penetrable volume fractions as the pore-size distribution and reported data for pore size [19,20]. These data are unrealisticly low [20] (as might be expected) when compared to earlier published results [22,23].

The situation was finally addressed by Knox and Scott [8] who pointed out the ambiguities of different approaches and who also derived an equation for calculating the pore size distribution from the selectivity curve. Hagel [24] derived a numerical expression for the Knox and Scott equation from a logit function of the calibration curve and applied this to different materials. However, at low pore radius anomalities of the resulting pore distribution curve was observed [24]. The same phenomenon using the Knox and Scott [25,26] method has been observed by other groups. Vilenchik et al. [27] also proposed a method for the calculation of the PSD from distribution coefficients. However, the method that resulted in triangular PSD curves of alumina materials was not explicitly described.

Freeman and Poinescu [28–30] used the pore models by Giddings et al. [31] to estimate the pore size from the plot of ln(distribution coefficient) versus solute size. Data for pore size from this method was reported [32] to be comparable to the procedure described by Halász.

A quite different approach was presented by Jerabek who calculated the retention volume from a given pore volume distribution and adjusted this distribution until acceptable agreement between experimental and calculated data for retention times was obtained [33]. However, the resolution was low due to the small number of points used in the calculation for the pore volume distribution. This principle was also suggested by Knox and Ritchie [34] to overcome the problem with the instability noticed in the earlier procedure. Gorbunov et al. presented an extensive review of what may be called "chromatographic porosimetry" [26]. They concluded that calculations of the PSD from the selectivity curve will suffer from instabilities due to experimental errors and that the preferred methodology is based upon the principle as outlined by Jerabek, and Knox and Ritchie [33,34].

The interpretation of size-exclusion data into pore size requires an assumption about the pore shape. Unfortunately, many materials have a rather complicated structure which may not be described accurately by a few parameters. The often used model of cylindrical pores may perhaps only be applicable to porous glass as described by Haller [35]. Laurent and Killander [4] used the Ogston model to describe the structure of cross-linked dextran in terms of concentration and radius of fibers making up the matrix. Giddings et al. [31] used statistical mechanics to relate size-exclusion of molecules of various shapes from porous networks of different structures. Van Kreveld and Van den Hoed [36] found good agreement between experiment and calculated distribution coefficients assuming a random sphere model of a silica-based matrix. Thus, from size-exclusion data useful information about the physical structure of the matrix may be obtained, provided that a relevant model for the structure is available. But this is seldom the case and simple geometric models may not be able to describe the irregular structure of the matrix properly [37]. Gorbunov et al. [26] suggested the use of the pore specific surface area since this is a pore-model independent characteristics.

However, methods used in material science for characterization of inorganic materials, e.g., silica, include mercury porosimetry and nitrogen sorption and these methods rely upon a cylindrical pore model for the interpretation of the results into pore dimensions [38,24]. It is therefore natural to, as a first attempt, use this pore model also for calculation of apparent pore dimensions of chromatographic material. This will facilitate comparisons with data

from, e.g., mercury porosimetry and furthermore will provide a figure that may be of conceptual value for choosing a gel with suitable SEC properties for the solute size at hand. Finally, it is obvious that using this model all data are apparent and may not be misinterpreted as depicting the physical texture of the matrix.

Here we evaluate a simple approach to the problem of relating the selectivity curve to an apparent pore size assuming a cylindrical pore shape. The basic principle is to assign a pore-size distribution to the material, calculate the theoretical selectivity curve, compare with the experimental selectivity curve and adjust the apparent pore size distribution until the difference between the calculated and the experimental data are minimized [33,34,26]. The influence of different pore shapes on the result was also studied.

Dextran was selected as probe molecules in this study, the reason being that dextran is a well-defined polymer and that the viscosity radius of dextran has been found to be a relevant size estimate for globular proteins [39–41].

2. Experimental

2.1. Chromatography

2.1.1. Materials

The separation media studied were traditional gel filtration media, e.g., Sepharose and Sephacryl, high-resolution media, e.g., Superose and the new high selectivity media Superdex (all from Pharmacia Biotech, Uppsala, Sweden). Fourteen samples of dextran and the glucose monomer were used in the study of column selectivity (Table 1). The eluent was 0.15 *M* NaCl solution.

2.1.2. Apparatus

Media were packed according to the manufacturers instruction in columns of dimensions 50×1.6 cm (HR 16/50; Pharmacia). The packed columns were qualified as judged by plate count test after packing yielding a reduced plate height of better than 3. An automatic injector (ACT-100; Pharmacia) and a peristaltic pump (P-1; Pharmacia) were used for automatic sample application. The effluent was continuously monitored with a refractometer (2142 differential refractometer, Pharmacia LKB). The flow-rate was controlled by a high-precision pump (P-500; Pharmacia). Data was collected with a computer interface (900 series interface; PE Nelson). The retention times were calculated using Turbochrom Navigator 4.0 (PE Nelson).

For some of the gels data were obtained from the calibration curve as described elsewhere [42]. For Superdex Peptide the selectivity curve was calculated from the individual components of Dextran 1.

Table 1
Data for the dextran standards

Sample	M_p[a]	R_η[b] (nm)	Conc. (mg/ml)
D-Glucose	180	(0.360)	0.75
Pharmacosmos 1	1 080	0.878	10
Pharmacosmos 5	4 440	1.76	10
Pharmacosmos 12	9 890	2.65	10
Pharmacosmos 25	21 400	3.89	10
Pharmacosmos 50	43 500	5.53	3.5
Pharmacosmos 80	66 700	6.45	2.3
Pharmacosmos 150	123 600	9.31	1.5
Pharmacosmos 270	196 300	11.7	1.5
Pharmacosmos 410	276 500	13.9	1.5
Pharmacosmos 670	401 300	16.7	1.5
Pharmacia $1.8\cdot10^6$	1 084 000	27.4	10
Pharmacia $4.97\cdot10^6$	3 292 000	47.7	10
Pharmacia $9.7\cdot10^6$	6 105 000	65.9	10
Blue dextran 2000	void		10

[a] M_p is the molecular mass corresponding to the peak as stated by the suppliers (Pharmacosmos, Viby, Denmark and Pharmacia, Uppsala, Sweden).
[b] The viscosity radius was calculated from $R_\eta = 0.0271 M_p^{0.498}$ [24].

2.2. Calculations

The molecular mass corresponding to the peak apex of the dextran sample was related to viscosity radius (in nm), from the equation given in Ref. [24]

$$R_\eta = 0.0271 \cdot M_p^{0.498} \quad (1)$$

The distribution coefficient was calculated from the retention volume corresponding to the peak apex, V_R, from

$$K_D = \frac{V_R - V_o}{V_t - V_o} \quad (2)$$

where V_0 is the void volume and V_t is the total liquid volume of the column.

The theoretical distribution coefficient was calculated from

$$K_D = \frac{\sum_R^\infty K \cdot f(r)\Delta r}{\sum_0^\infty f(r)\Delta r} \quad (3)$$

where K is the local distribution coefficient and $f(r)$ is the relative volume fraction of pores as a function of pore size, i.e., the differential pore size distribution. A Gaussian distribution of pore sizes, with a mean of r_p and standard deviation of s_p, was used and $f(r)$ calculated from

$$f(r) = \exp\left[-\frac{1}{2}\left(\frac{r - r_p}{s_p}\right)^2 \right] \quad (4)$$

The local distribution coefficient, K, is given for different pore shapes by

$$K = (1 - R/r)^a \quad (5)$$

where R is the effective radius of the solute (here equal to the viscosity radius, see Section 4), r is the effective radius of the pore and a is a pore-shape-dependent constant, being equal to 1 for slab, 2 for cylindrical and 3 for spherical pores [47].

The calculations were performed using Excel (Microsoft) and the values for mean effective radius and variance of the pore size distribution that minimized the differences between experimental and theoretical distribution coefficient were found by using the "Solver" in Excel. Start values for the iteration procedure was $r_p = 3R_\eta$ and $s_p = R_\eta/2$ calculated from the solute radius at $K_D = 0.5$. The calculation was performed at a resolution of 100 datapoints with $\Delta r \approx 6 \cdot s_p/100$.

3. Results

3.1. Comparison with nitrogen sorption data

The procedure was first tested by analyzing size-exclusion data for polystyrene on a silica based material for which result from nitrogen sorption was available. The experimental data was taken from Ref. [24]. The resulting selectivity curve as compared to the experimental curve is shown in Fig. 1. The selectivity curve from a hypothetical support having a cylindrical pore shape with a radius of 23 nm and a Gaussian distribution of pore sizes with a standard deviation of 7 nm yields good agreement with experimental size-exclusion chromatography data. The apparent pore size distribution is in fair agreement with data from nitrogen sorption, as shown in Fig. 2. This figure also displays a variability in data from nitrogen sorption at low pore radius. It is interesting to note that the width of the apparent pore size distribution is in good agreement with nitrogen sorption data.

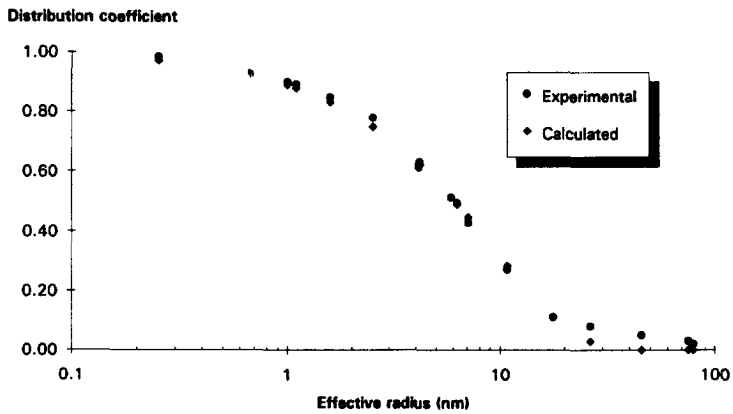

Fig. 1. Selectivity curve for silica gel using SEC of polystyrene standards and calculated with the presented procedure assuming $r_p = 23$ nm, s_p 17 nm. Experimental data from Ref. [24].

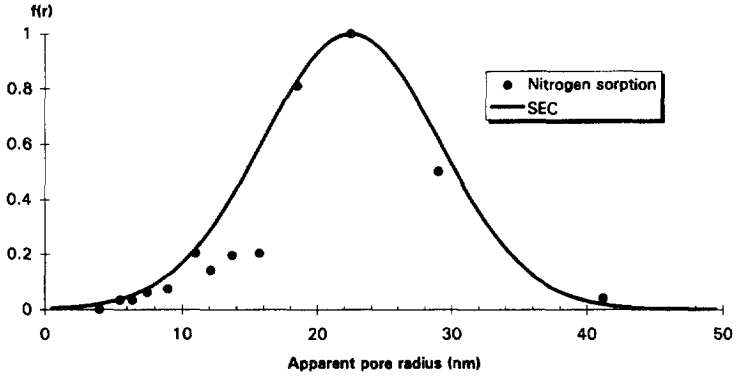

Fig. 2. Comparison of apparent PSD from experiment in Fig. 1 with data from nitrogen sorption.

3.2. Comparison with the Knox and Scott equation

In Fig. 3 the result of the present approach is compared to the complicated relationship derived by Hagel [24] using the equation proposed by Knox and Scott [8]. The agreement between the two approaches is fair, in consideration that truncation of negative data in the application of the equation will result in a slight skew of data [25,26].

3.3. Method accuracy and variability

Fig. 2 indicates that the proposed method yields results in agreement with an independent method (with both methods assuming a cylindrical pore shape). The precision of the determination was tested by repeating the entire procedure tree times. The maximal variation in apparent pore radius from the mean value was found to be 2% for the most sensitive case (i.e., when the apparent pore size distribution is extremely narrow). The effect of deleting data points was tested systematically. We found that a symmetrical reduction of data points from 20 to 7 had a very small effect on the calculated pore size distribution. However, large effects were noted when data points were missing in the central region of the selectivity curve (i.e., $0.25 < K_d < 0.75$). On the other hand, data covering this central region was sufficient to yield consistent values of the apparent pore size distribution, see

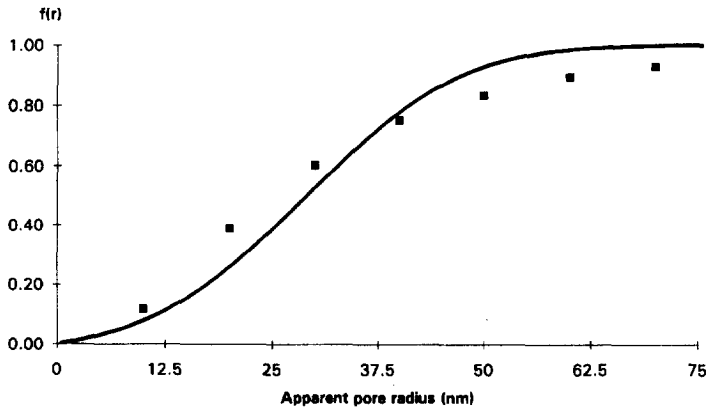

Fig. 3. Size-exclusion pore dimension of Superose 6 as obtained by the presented approach (———) and from derivation via the Knox and Scott equation with experimental data taken from Ref. [24] (■). Sample: dextran fractions.

Table 2. Thus, the method seems to be very robust, provided experimental data covers the central part of the selectivity curve.

3.4. Size-exclusion dimensions of Superdex peptide and pore structure

Fig. 4 shows the result from applying the procedure to a high selectivity material. The apparent cylindrical pore dimension is found to be 13 nm and the material separates molecules as though the pore dimension is uniform. However, it is important to point out that this does only depict the functional performance of the material and not the true physical dimensions of the pores. In this case the desired effect is caused by grafting dextran chains of suitable size and concentration to the agarose back bone to create an environment where the entropy is drastically reduced for molecules larger than 13 nm. The figure also shows that the exclusion data may be fitted to other types of pore geometries, giving quite different estimates of the apparent pore dimension. This is not surprising and the dimensions should, in theory, be related by 1:2:3 for slab:cylinder:sphere [26]. The result illustrates that in order to obtain meaningful physical information from apparent pore size a realistic pore model is needed a priori.

3.5. Size-exclusion dimensions of gel filtration media

The size-exclusion pore dimensions of various media found by this method are compiled in Table 3. Data found in literature are also given for purpose of comparisons. It should be noted that, since data refer to different lots, it cannot be expected that the values

Table 2
Effect of deleting data points on the calculated pore dimensions

R_η, (nm)	K_D	Data points included (as marked with x)									
		1	2	3	4	5	6	7	8	9	10
37.6	0.02	x	x	x	x		x	x			x
30.1	0.06	x			x		x	x			x
24.5	0.09	x	x		x	x	x	x			x
18.0	0.15	x		x		x	x	x			x
14.5	0.20	x	x				x	x			x
11.9	0.25	x					x	x	x		
9.9	0.30	x	x	x	x	x	x	x	x		
8.4	0.35	x			x	x	x	x	x		
6.9	0.41	x	x		x		x	x	x		
6.1	0.45	x		x				x	x		
5.2	0.50	x	x			x		x	x	x	
4.4	0.55	x				x			x	x	
3.7	0.60	x	x	x	x				x	x	
3.2	0.65	x			x				x	x	
2.6	0.70	x	x		x	x			x	x	
2.1	0.75	x		x		x			x	x	
1.7	0.80	x	x							x	x
1.3	0.85	x								x	x
0.9	0.90	x	x	x	x	x				x	x
0.6	0.95	x			x	x				x	x
0.4	1.00	x	x		x					x	x
Apparent dimensions											
r_p (nm)		20.9	20.9	20.5	21.6	21.6	23.9	22.6	20.5	19.7	27.7
s_p (nm)		10.4	10.4	10.2	10.8	10.8	12.0	11.3	10.2	8.8	13.8

In this study K_D for glucose was arbitrarily set to 1; this may yield 0.4 nm too high estimate of apparent dimensions as discussed in text. However, the conclusions drawn are not affected. Data points were taken from a calibration curve for Superose 6 prep grade using dextran samples and the procedure described in Ref. [42].

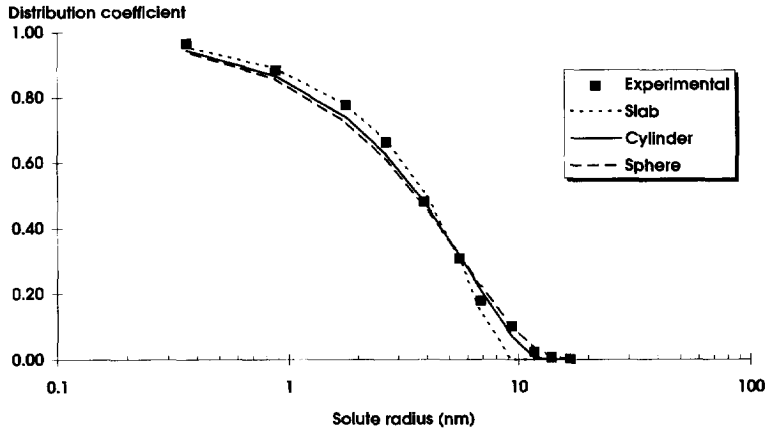

Fig. 4. Selectivity curve calculated for different pore models. Experimental data: dextran fractions on Superdex 200. Best fit to data using different pore models according to Eq. 5 yields: $r_p = 8.0$ nm and $s_p = 0.1$ nm for slab (– – – –); $r_p = 12.7$ nm and $s_p = 0.1$ nm for cylinder (———); and $r_p = 17.4$ nm and $s_p = 0.1$ nm for sphere (— — —).

should coincide. In spite of this it may be noticed that data from different sources, albeit sparse, support the results given here. It may be noted that the choice of solute for determination of the total pore volume will require special considerations, especially for media of low pore dimensions. The size of glucose may be expected to add 0.4 nm to the estimated radius if not corrected for. Data in Table 3 are corrected for this effect.

Table 3
Size-exclusion pore dimensions of gel filtration media

Gel type	Size-exclusion pore dimension (nm)	Reference
Sepharose CL 2B	75	
Sepharose CL 4B	42	
Sepharose 4 FF	45	
Sepharose CL 6B	24	
Sepharose 6 FF	29	
Superose 6 prep grade	21	
Superose 6	25	
Superose 6	29	
Superose 6	25	[22]
Superose 12	10	
Superose 12	14	[22]
Superose 12	12	[41]
Sephacryl S-400 HR	31	
Sephacryl S-300 HR	13	
Sephacryl S-200 HR	7.7	
Sephacryl S-100 HR	6.6	
Superdex 200	13	
Superdex 75	6.0	
Superdex 30 prep grade	3.8	
Superdex Peptide	3.3	

4. Discussion

4.1. Effective size of dextran

The model used assumes that the size of the solute used may be regarded as a hard sphere of a certain effective size [8]. The effective size of dextran was taken as the viscosity radius as given in Ref. [24]. The rationale for this choice is the experimental findings that dextran and globular proteins are eluted according to equal viscosity radius in size-exclusion chromatography, irrespective of gel matrix used [39–41]. The viscosity radius differs from the radius of gyration of dextran with a factor of 0.8 to 0.9 in the size range 0.2–8.5 nm [24,43]. This is in good agreement with the calculation of effective size of a fluctuating random coil from radius of gyration [36]. It may be argued that the application of the hard sphere model is not formally correct since the probe molecules used, i.e., dextran, are flexible and may permeate pores smaller than their nominal size [26]. We, therefore, calculated the apparent radius of Ficoll fractions analyzed by SEC. Ficoll can be regarded as spherical non compact molecule [44]. As

Table 4
Molecular size of Ficoll from light scattering and dextran calibration

Fraction	Light scattering			Dextran calibration		
	M_w	M_n	R_{St}^a (nm)	M_p	K_d	R_η^b (nm)
1	175 530	146 060	7.3	75 070	0.36	7.3
2	105 210	93 240	5.9	49 780	0.46	5.9
3	60 710	52 750	4.6	32 230	0.55	4.8
4	37 360	31 720	3.8	20 670	0.62	3.8
5	21 290	17 460	3.0	13 920	0.69	3.1

[a] Stokes radius calculated from $R_{St}=0.0421M_w^{0.427}$ according to Ref. [45] (M_w and M_n were determined by DAWN laser photometer after SEC on Superose 6).
[b] The viscosity radius was calculated from the molecular weight corresponding to the peak using dextran calibration and $R_\eta=0.0271M_p^{0.498}$ [24].

seen from Table 4 there is good agreement between the effective radius calculated from the dextran calibration curve and data from light scattering and, furthermore, no trends in data for the two methods as function of size were seen. This may be because the effect of polymer chains entering into small pores is negligible for the pore structures of the media used for these investigations or that the effect is small in the range studied in this and other work. Thus, we conclude that the viscosity radius of dextran is suitable as a measure of the effective size of a hard sphere at least within the range $0.36<K_d<0.69$. Furthermore, it must be pointed out that the major uncertainties in determination of pore dimension arises from the selection of pore model.

4.2. Pore shape

The ability of SEC to differentiate between different pore shapes was tested by fitting experimental data to three different pore models (i.e., setting $a=1$, 2 or 3 in Eq. 5) yielding quite different suggestions of apparent pore size as seen in Fig. 4. Furthermore, there is no obvious preference for any of the pore shapes from these data. Thus, unless we have a reliable pore structure it is not possible to get structural information from size-exclusion chromatography. However, we do get functional information which may be useful to predict separations and also for comparisons between materials. However, to stress that the information obtained may not be the correct pore size we suggest the use of the terminology apparent pore size or perhaps more suitable, size-exclusion dimensions, to describe data obtained on matrices of unknown pore structure (or in the general case where reference to other methods, e.g., mercury porosimetry or nitrogen sorption is not made, data may be expressed in terms of pore specific surface area).

The simple procedure outlined in this work is applicable for the purpose of obtaining estimates of apparent size-exclusion dimensions of a porous matrix (i.e., what size of solutes the gel will accommodate). However, it must be stressed that the interpretation of the data into equivalent dimensions of a cylindrical shape is merely for intuitive purpose and to facilitate comparisons with established methods. This is illustrated by the structure of Sephacryl S-500 as depicted by scanning electron microscopy in Fig. 5. Evidently no spherically-shaped pores are noted.

It may be pointed out that the procedure is applicable to any pore model, i.e., as long as numerical expressions can be given for $f(r)$ and K, and in this sense the procedure is generally applicable to all types of matrices.

4.3. Use of proteins

One of the incentives for this study was a recent report where the authors used proteins to characterize the selectivity of size-exclusion media [20]. The selectivity was modeled from the sum of two Gaussian function and finally the selectivity curve was set equal to the pore-size distribution. The procedure suffers from two shortcomings. Firstly, proteins do not represent a homologous series of molecules and their shape may vary substantially. Furthermore, interactions with the gel medium may be experienced which will affect the results severely [46]. Secondly, setting the pore-size distribution equal to the selectivity curve is formally incorrect [8]. Subsequently, the estimations of pore size dimensions were not in accordance with published data (e.g., Sephacryl S-300 was claimed to have two pore-size distributions with mean values of 1.75 and 5.97 nm). We, therefore, tested our approach to the data given in Fig. 1 in Ref. [20]. The result is shown in Fig. 6 which

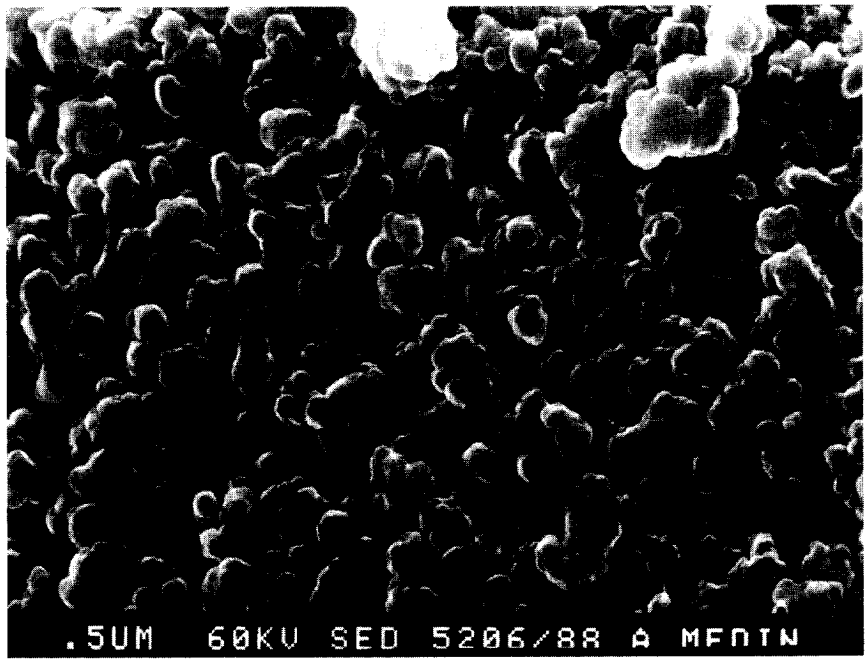

Fig. 5. Scanning electron micrograph of Sephacryl S-500. Magnification 25 000×.

shows the fit of experimental data to a material having a size-exclusion dimension of 13 nm which is in excellent agreement with data found with dextran for this type of gel (Table 3). Furthermore, an attempt to force a bimodal PSD to the experimental data gave not better fit to data points. This is not surprising, since SEC is inherently rather insensitive to pore shape [26]. It may be concluded that the interpretation of SEC data into a bimodal pore-size distribution is not supported by this method and may, furthermore, be attributed to the use of inappropriate methodology.

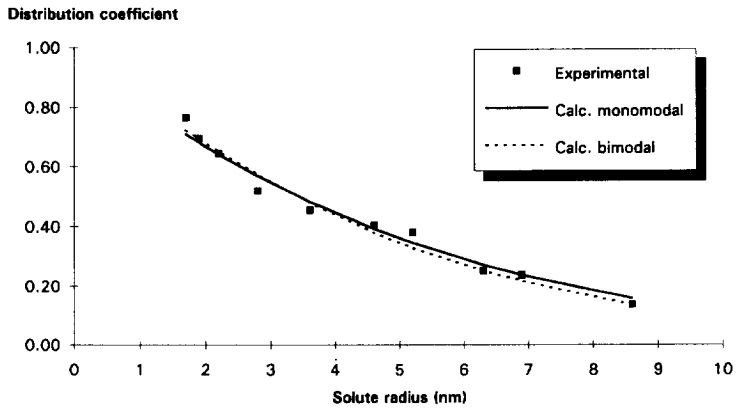

Fig. 6. Selectivity curve for proteins on Sephacryl S-300 HR. Experimental data taken from Ref. [20]. Data for monomodal size distribution calculated for a cylindrical pore shape with $r_p = 13.2$ nm and $s_p = 6.7$ nm. Forced bimodal distribution gave $r_{p1} = 13.2$ nm, $s_{p1} = 4.4$ nm, and $r_{p2} = 12.5$ nm and $s_{p2} = 6.3$ nm for best fit.

5. Conclusions

The apparent size-exclusion pore dimensions of porous media may be determined by a simple application of Excel. The procedure is robust and yields results in good agreement with published data. It is important that inert solutes belonging to a homologous series is used as probes, e.g., dextran for aqueous size-exclusion media. Data for gel filtration media may be fitted to a Gaussian pore size distribution using a cylindrical pore model. Information about the physical pore structure of chromatography media may currently not be obtained by SEC.

References

[1] B. Lindqvist and T. Storgårds, Nature, 175 (1955) 511.
[2] G.H. Lathe and C.R.J. Ruthven, Biochem. J., 62 (1956) 665.
[3] J. Porath and P. Flodin, Nature, 183 (1959) 1657.
[4] T.C. Laurent and J. Killander, J. Chromatogr., 14 (1964) 317.
[5] L.G. Aggebrandt and O. Samulesson, J. Appl. Polym. Sci., 8 (1964) 2801.
[6] J. Porath, Pure Appl. Chem., 6 (1963) 233.
[7] A.J. de Vries, M. Le Page, R. Beau and C.L. Guillemin, Anal. Chem., 39 (1967) 935.
[8] J.H. Knox and H.P. Scott, J. Chromatogr., 316 (1984) 311.
[9] I. Halász and K. Martin, Ber. Bunsenges. Phys. Chem., 79 (1975) 731.
[10] I. Halász and K. Martin, Angew. Chem., Int. Ed. Engl. 17 (1978) 901.
[11] R. Nikov, W. Werner and I. Halász, J. Chromatogr. Sci., 18 (1980) 207.
[12] W. Werner and I. Halász, J. Chromatogr. Sci., 18 (1980) 277.
[13] T. Crispin and I. Halász, J. Chromatogr., 239 (1982) 351.
[14] O. Schou, L. Gotfried and P. Larsen, J. Chromatogr., 254 (1983) 289.
[15] B. Gelleri and M. Sernetz, Anal. Chim. Acta, 163 (1984) 17.
[16] F. Nevejans and M. Verzele, Chromatographia, 20 (1985) 173.
[17] S. Kuga, J. Chromatogr., 206 (1981) 449.
[18] M. Andersson, A. Axelsson and G. Zacchi, Bioseparations, 5 (1995) 65.
[19] M. le Maire, A. Ghazi, J.V. Moller and L.P. Aggerbeck, Biochem. J., 243 (1987) 399.
[20] J.E. Harlan, D. Picot, P.J. Loll and R.M. Garavito, Anal. Biochem., 224 (1995) 557.
[21] G.K. Ackers, J. Biol. Chem., 242 (1967) 3237.
[22] M Potschka, J. Chromatogr., 648 (1993) 41.
[23] K.K. Unger, B. Anspach and H. Giesche, J. Pharm. Biomed. Anal., 2 (1984) 139.
[24] L. Hagel in P.L. Dubin (Editor) Aqueous Size-Exclusion Chromatography, Elsevier, Amsterdam, 1988, p. 119.
[25] O. Schou, P. Larsen, V. Bodstrup and I. Rohde, presented at the 12th International Symposium on Column Liquid Chromatography, Washington, DC, 19–24 June 1988.
[26] A.A. Gorbunov, L.Ya. Solovyova and V.A. Pasechnik, J. Chromatogr., 448 (1988) 307.
[27] L.Z. Vilenchik, J. Asrar, R.C. Ayotte, L. Ternorutsky and C.J. Hardiman, J. Chromatogr., 648 (1993) 9.
[28] D.H. Freeman and I.C. Poinescu, Anal. Chem., 49 (1977) 1183.
[29] S.B. Schram and D.H. Freeman, J. Liq. Chromatogr., 3 (1980) 403.
[30] D.H. Freeman and S.B. Schram, Anal. Chem., 53 (1981) 1235.
[31] J.C. Giddings, E. Kucera, C.P. Russell and M.N. Myers, J. Phys. Chem., 72 (1968) 4397.
[32] O. Chiantore and M. Guaita, J. Chromatogr., 260 (1983) 41.
[33] K. Jerábek, Anal. Chem., 57 (1985) 1595.
[34] J.H. Knox and H. Ritchie, J. Chromatogr., 387 (1987) 65.
[35] W. Haller, Nature, 206 (1965) 693.
[36] M.E. van Kreveld and N. van den Hoed, J. Chromatogr., 83 (1973) 111.
[37] M. Kubín and S. Vozka, J. Appl. Polym. Sci. Polym. Symp., 68 (1980) 209.
[38] K. Unger, Angew. Chem., Int. Ed. Engl., 11 (1972) 267.
[39] R.P. Frigon, J.K. Leypoldt, S. Uyeil and L.W. Hendersson, Anal. Chem. 55 (1983) 1349.
[40] L. Hagel, A. Hartmann and K. Lund, J. Chromatogr., 641 (1993) 63.
[41] P.L. Dubin and J.M. Principi, Macromolecules, 22 (1989) 1891.
[42] G. Nilsson and K. Nilsson, J. Chromatogr., 101 (1974) 137.
[43] K.A. Granath, J. Colloid. Sci., 13 (1958) 308.
[44] P.L. Dubin, Carbohydr. Polym., 25 (1994) 295.
[45] J.D. Oliver III, S. Anderson, J.L. Troy, B.M. Brenner and W.M. Deen, J. Am. Soc. Nephrol., 3 (1992) 214.
[46] S. Hussain, M.S. Mehta, J.I. Kaplan and P. Dubin, Anal. Chem., 63 (1991) 1132.
[47] W.W. Yau and D.D. Bly, in T. Provder (Editor), Size Exclusion Chromatography (GPC) (ACS Symposium Series, No. 138), American Chemical Society, Washington, DC, 1980, pp. 197–206.